ISSN (Print) 1226-1750
ISSN (Online) 2233-6656
Journal of Magnetics 24(3), 392-401 (2019) https://doi.org/10.4283/JMAG.2019.24.3.392

Comparison of Magnetic Force Calculation on Permanent Magnets with Models of Equivalent Magnetic Charge and Magnetizing Current

Yuyang Zhang[1], Yonggang Leng[1]*, Jinjun Liu[2], and Dan Tan[3]

[1]*School of Mechanical Engineering, Tianjin University, Tianjin 300350, China*
[2]*School of Control and Mechanical Engineering, Tianjin Chengjian University, Tianjin 300384, China*
[3]*Beijing Institute of Nanoenergy and Nanosystems, Chinese Academy of Sciences, Beijing 100083, China*

(Received 1 November 2018, Received in final form 23 August 2019, Accepted 27 August 2019)

Accurate magnetic force calculation is essential to effectively analyzing a system or device containing magnets. Among several approaches used in the interacting magnetic force calculation of permanent magnets, equivalent magnetic charge and equivalent magnetizing current models are widely adopted. In this paper, we choose cubes and cylinders as calculating objects to investigate the detailed calculation procedures. Higher calculation accuracy of the equivalent magnetizing current model is verified by comparison between simulation and experiment results. Furthermore, we analyze the relations between two models and discriminate their equivalence in the magnetic force calculation respectively at both micro and macro scale. Reference basis for choosing a proper model to calculate magnetic force is provided in this work, which is beneficial for the design of electro-mechanical structures with permanent magnets.

Keywords : permanent magnet, magnetic force calculation, equivalent magnetizing current, equivalent magnetic charge

1. Introduction

Nowadays, considerable attention has been paid to the electro-mechanical system and the robotic technology. Magnets are widely used in electro-mechanical structures like motors and relays. and some frontier researches such as vibration energy harvesting system [1-4]. As a non-contact force, magnetic force is appropriate for some particular situations such as valves and pumps [5, 6]. Meanwhile, high energy densities of magnets are attractive in micro-scale devices due to the nonlinearity of magnetic force. Numerous researchers have been devoted to exploring the dynamic character of the vibration energy harvesting system in which magnets participate. In order to improve energy harvesting efficiency, it is advantageous to realize nonlinear bi-stable or multi-stable energy harvester with magnetic force. To this end, the accurate magnetic force calculation is of key importance for an effective analysis of a system or device with magnets [7-10].

Although there exist several approaches calculating magnetic force between permanent magnets [11-14], how to choose the most appropriate model still requires further research. We focus on the two most popular and accessible models based on the equivalent magnetic charge and the magnetizing current [5, 15], respectively, to figure out their differences and relations.

Experiments are firstly set up to measure the actual forces between permanent magnets. Two typical shapes of magnets, cuboid and cylinder, are chosen because of their wide applications and easily manufacturing in commercial realm [16]. We fully analyze magnetic force between permanent magnets with both of these two theories, equivalent magnetic charge and equivalent magnetizing current. Expressions of magnetic force are demonstrated in detail then. Comparison results indicate that the equivalent magnetizing current model has higher accuracy than that of equivalent magnetic charge model. Furthermore, we investigate the relations between these two models and their calculation equivalence are distinguished at different scales.

*Corresponding author: Tel: +86(0)2227403285
Fax: +86(0)2227403285, e-mail: leng_yg@tju.edu.cn

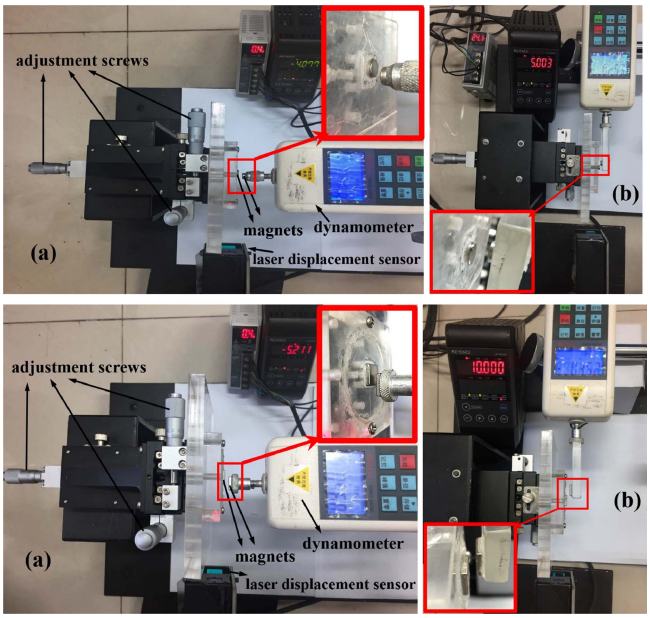

Fig. 1. (Color online) Magnetic force measurement system. (a) axial force between cylindrical magnet pair, (b) lateral force between cylindrical magnet pair, (c) axial force between cuboid magnet pair, (d) lateral force between cuboid magnet pair.

2. Experimental Details

Before building models to calculate magnetic forces, an experiment is designed to measure the actual position-dependent magnetic forces between permanent magnets, as shown in Fig. 1. Here, a pair of 10 mm × 10 mm × 2 mm N38H $Nd_2Fe_{14}B$ cuboid magnets and a pair of Φ6 mm × 2 mm N38H $Nd_2Fe_{14}B$ cylindrical magnets are chosen to be the measured objects in the experiment. One magnet of each pair is attached to the adjusted platform and the other one to the dynamometer (HF-5). The like magnetic poles are arranged face to face, which means the axial repulsive magnetic forces exist between the magnet pairs in this experiment. We adjust the screws to simulate different relative positions of the magnets, while recording the displacements and forces in the laser displacement sensor (LK-G5001V) and dynamometer, respectively, whose minimum resolutions are 0.001 mm and 0.001 N. Parts of the obtained experimental data of position-dependent interacting magnetic forces are shown as dots in the figures of Tables 1 and 2 in Sec. IV.

3. Magnetic Force Calculations

3.1. Equivalent magnetic charge theory

The equivalent magnetic charge theory is based on the magnetic dipole model as its micro model. It states that

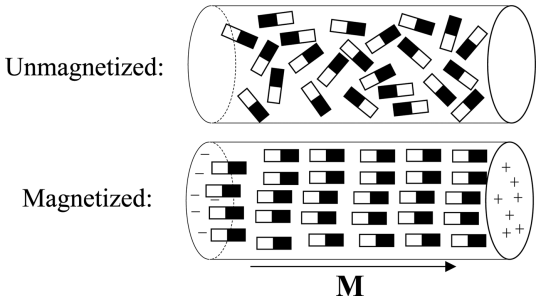

Fig. 2. Schematic drawing of the equivalent magnetic charge model. (Same as cuboid magnet)

the magnetic charges gather in the surfaces of magnetic poles. An unmagnetized permanent magnet has no magnetism at macro scale, because the magnetic dipolar molecules are random in the magnet and the magnetic dipole moments are offset by each other. Whereas a magnetized permanent magnet has north and south poles only on the two end faces, due to the organized arrangement of interior magnetic dipolar molecules, where the north and south poles link one after another along the direction of magnetic field. It means that positive and negative magnetic charges only distribute on the surfaces of magnetic north and south poles, as shown in Fig. 2 [17]. The interactions between permanent magnets could be equivalent to that among these magnetic charges, for both produced magnetic field and acting magnetic force.

The equivalent magnetic charge model of permanent magnet is obtained by solving the Maxwell equations with the introduction of scalar magnetic potential [18]. The scalar magnetic potential equation of an arbitrary point P in the magnetic field produced by a magnetic dipole (charge) is $U_m = \frac{1}{4\pi\mu_0}\frac{\boldsymbol{P}_m \bullet \hat{\boldsymbol{r}}}{r^2}$, similar to the electrical field produced by an electric charge, where $\boldsymbol{P}_m = p_m \boldsymbol{l}$ is the magnetic dipole moment, $\hat{\boldsymbol{r}}$ is a unit

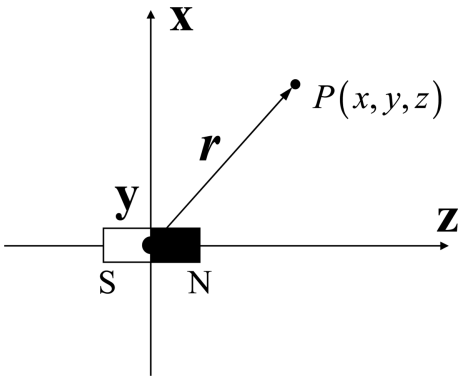

Fig. 3. Magnetic field of an arbitrary point in space produced by a single magnetic dipole magnetized in the z-axis.

vector of the vector $\boldsymbol{r}$ from the charge to the arbitrary point P and μ_0 is permeability of vacuum. The expressions of magnetic field intensities can be derived from the scalar magnetic potential.

3.1.1. Cuboid magnets

We use a coordinate system as shown in Fig. 3 with its origin located at the core point of magnetic dipole. The magnetic dipole p_m is magnetized in the z-axis. The scalar magnetic potential at an arbitrary point $P(x, y, z)$ thus has the following form:

$$U_m = \frac{p_m}{4\pi\mu_0}\frac{z}{(x^2+y^2+z^2)^{3/2}}. \tag{1}$$

The magnetic field of a single charge at an arbitrary point $P(x, y, z)$ could be determined as $\boldsymbol{H} = -\nabla U_m$. So the magnetic field intensities produced by one magnetic charge in x, y, and z directions respectively are:

$$\begin{aligned} H_x &= -\frac{\partial U_m}{\partial x} = \frac{p_m}{4\pi\mu_0}\frac{3xz}{(x^2+y^2+z^2)^{5/2}} \\ H_y &= -\frac{\partial U_m}{\partial y} = \frac{p_m}{4\pi\mu_0}\frac{3yz}{(x^2+y^2+z^2)^{5/2}} \\ H_z &= -\frac{\partial U_m}{\partial z} = \frac{p_m}{4\pi\mu_0}\frac{2z^2-y^2-x^2}{(x^2+y^2+z^2)^{5/2}} \end{aligned}. \tag{2}$$

The force acting on a charge in the external magnetic field is

$$\boldsymbol{F} = p_m\boldsymbol{H}, \tag{3}$$

where $p_{mA} = \sigma_{sA}dqdt$, and $p_{mB} = \sigma_{sB}dhdw$. A permanent magnet is equivalent to a model of accumulated magnetic charges, composing of a volume charge density $\sigma_v = -\mu_0 dlv\boldsymbol{M}$ and a surface charge density $\sigma_s = \mu_0(\boldsymbol{n}\cdot\boldsymbol{M})$. The volume charge density is zero for a magnet magnetized uniformly with a constant $\boldsymbol{M}$ and the surface charge densities are given by $\sigma_{sA} = \mu_0 M_A$ and $\sigma_{sB} = \mu_0 M_B$ [19]. The interacting force between two square magnetic pole faces covered with positive or negative magnetic charges is achieved by using twice surface integrals as

$$\begin{aligned} &\boldsymbol{F}_{mn}(x,y,z) = \\ &\pm\frac{\sigma_{sA}\sigma_{sB}}{4\pi\mu_0}\int_{-\frac{h_A}{2}}^{\frac{h_A}{2}}\int_{-\frac{w_A}{2}}^{\frac{w_A}{2}}\int_{-\frac{h_B}{2}}^{\frac{h_B}{2}}\int_{-\frac{w_B}{2}}^{\frac{w_B}{2}}\frac{3(x+q-h)z}{\left((x+q-h)^2+(y+t-w)^2+z^2\right)^{5/2}}dwdhdtdq\boldsymbol{i} \\ &\pm\frac{\sigma_{sA}\sigma_{sB}}{4\pi\mu_0}\int_{-\frac{h_A}{2}}^{\frac{h_A}{2}}\int_{-\frac{w_A}{2}}^{\frac{w_A}{2}}\int_{-\frac{h_B}{2}}^{\frac{h_B}{2}}\int_{-\frac{w_B}{2}}^{\frac{w_B}{2}}\frac{3(y+t-w)z}{\left((x+q-h)^2+(y+t-w)^2+z^2\right)^{5/2}}dwdhdtdq\boldsymbol{j}, \\ &\pm\frac{\sigma_{sA}\sigma_{sB}}{4\pi\mu_0}\int_{-\frac{h_A}{2}}^{\frac{h_A}{2}}\int_{-\frac{w_A}{2}}^{\frac{w_A}{2}}\int_{-\frac{h_B}{2}}^{\frac{h_B}{2}}\int_{-\frac{w_B}{2}}^{\frac{w_B}{2}}\frac{2z^2-(y+t-w)^2-(x+q-h)^2}{\left((x+q-h)^2+(y+t-w)^2+z^2\right)^{5/2}}dwdhdtdq\boldsymbol{k} \end{aligned} \tag{4}$$

where h_A, h_B, w_A and w_B in the Eq. (4) denote the heights and widths of two square magnetic pole faces; d is the interval between the magnets; l_A and l_B are going to denote the thickness of magnets, as shown in Fig. 4. The magnets are placed in the way that their poles are faced to each other.

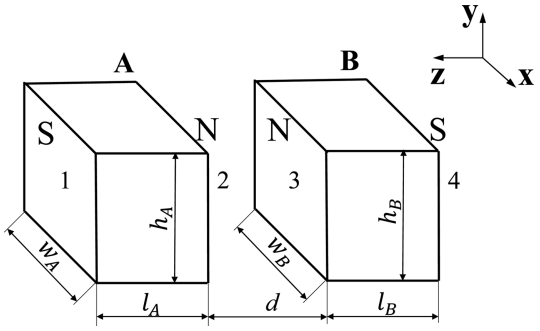

Fig. 4. Schematic diagram of geometric dimensions and interval between two cuboid magnets.

Hence, the interacting force between cuboid magnets is a sum of the contribution from both magnetic poles faces of two permanent magnets.

$$\begin{aligned} \boldsymbol{F} = &\boldsymbol{F}_{23}(x,y,d) + \boldsymbol{F}_{14}(x,y,d+l_A+l_B) \\ &-\boldsymbol{F}_{13}(x,y,d+l_B) - \boldsymbol{F}_{24}(x,y,d+l_A) \end{aligned}. \tag{5}$$

3.1.2. Cylindrical magnets

For a pair of cylindrical magnets, the basic theory of equivalent magnetic charge is the same as that of cuboid magnets above.

We use relations $y = r\cos\theta$ and $x = r\sin\theta$ to transform the Cartesian coordinate system to a cylindrical coordinate system as shown in Fig. 5. The magnetic field intensity produced by a single magnetic charge in three directions can be written as:

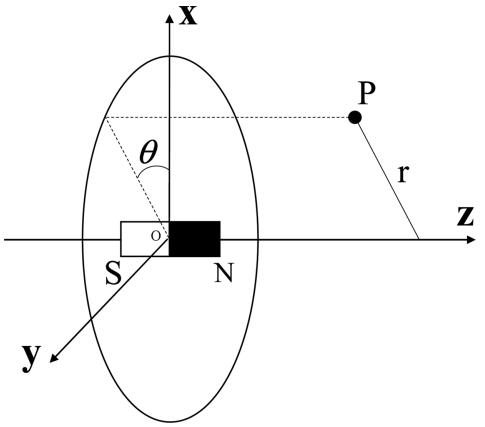

Fig. 5. Magnetic field of an arbitrary point in space produced by a single magnetic dipole in a cylindrical coordinate system.

$$H_x(r,\theta,z)=\frac{p_m}{4\pi u_0}\frac{3zr\sin\theta}{\left((r\sin\theta)^2+(r\cos\theta)^2+z^2\right)^{5/2}}$$
$$H_y(r,\theta,z)=\frac{p_m}{4\pi u_0}\frac{3zr\cos\theta}{\left((r\sin\theta)^2+(r\cos\theta)^2+z^2\right)^{5/2}}. \quad (6)$$
$$H_z(r,\theta,z)=\frac{p_m}{4\pi u_0}\frac{2z^2-(r\cos\theta)^2-(r\sin\theta)^2}{\left((r\sin\theta)^2+(r\cos\theta)^2+z^2\right)^{5/2}}$$

Similar to cuboid magnet's force, the axial and lateral interacted magnetic forces F_{zmn} and F_{rmn} between two circular magnetic pole faces covered with positive or negative magnetic charges are also obtained by using twice surface integrals,

$$F_{zmn}(z,r,\theta)=\pm\int_0^{r_B}\int_0^{2\pi}\int_0^{r_A}\int_0^{2\pi}\frac{\rho D\sigma_{m1}\sigma_{m2}}{4\pi}\frac{\begin{pmatrix}2z^2-(r\cos\theta+D\cos\beta-\rho\cos\alpha)^2\\-(r\sin\theta+D\sin\beta-\rho\sin\alpha)^2\end{pmatrix}}{\left(\begin{pmatrix}(r\sin\theta+D\sin\beta-\rho\sin\alpha)^2\\+(r\cos\theta+D\cos\beta-\rho\cos\alpha)^2+z^2\end{pmatrix}^{5/2}\right)}d\beta dDd\alpha d\rho$$
$$F_{rmn}(z,r,\theta)=\pm\int_0^{r_B}\int_0^{2\pi}\int_0^{r_A}\int_0^{2\pi}\frac{\rho D\sigma_{m1}\sigma_{m2}}{4\pi}\frac{\begin{pmatrix}3z(r\sin\theta+D\sin\beta-\rho\sin\alpha)\\or\ 3z(r\cos\theta+D\cos\beta-\rho\cos\alpha)\end{pmatrix}}{\left(\begin{pmatrix}(r\sin\theta+D\sin\beta-\rho\sin\alpha)^2\\+(r\cos\theta+D\cos\beta-\rho\cos\alpha)^2+z^2\end{pmatrix}^{5/2}\right)}d\beta dDd\alpha d\rho \quad (7)$$

where the indications of parameters ρ, α, θ, D and β are shown in Fig. 6. In the equation of F_{rmn}, the numerator could be written as $3z(r\sin\theta+D\sin\beta-\rho\sin\alpha)$ or $3z(r\cos\theta+D\cos\beta-\rho\cos\alpha)$, which represent magnetic force in x or y direction respectively. They have the same values after integral on account of the symmetry of a circular section.

The interacting magnetic force between two cylindrical permanent magnets is the sum of the contribution from both circular magnetic pole faces, that is

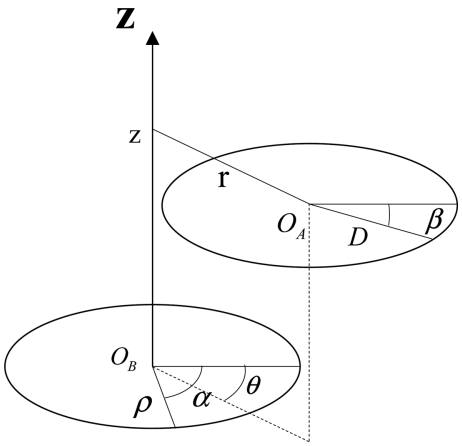

Fig. 6. Schematic diagram of calculation model of magnetic force between two circular magnetic pole faces.

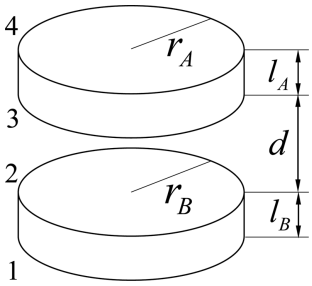

Fig. 7. Schematic diagram of geometric dimensions and interval between two cylindrical magnets.

$$\begin{aligned}F_z&=F_{z23}(d,r,\theta)+F_{z14}(d+l_A+l_B,r,\theta)\\&\quad-F_{z13}(d+l_B,r,\theta)-F_{z24}(d+l_A,r,\theta)\\F_r&=F_{r23}(d,r,\theta)+F_{r14}(d+l_A+l_B,r,\theta)\\&\quad-F_{r13}(d+l_B,r,\theta)-F_{r24}(d+l_A,r,\theta)\end{aligned}, \quad (8)$$

where d is the interval between magnets; l_A and l_B denote the thickness of magnets, as shown in Fig. 7. F_z and F_r represent the axial and lateral magnet force between permanent cylindrical magnets, respectively.

3.2. Equivalent magnetizing current theory

The theory of magnetizing current believes that magnetizing currents will exist inside the material and also on its surface magnetizing currents after the ferromagnetic material is magnetized in a magnetic field. For a uniformly magnetized permanent magnet whose magnetization intensity $\boldsymbol{M}$ is constant, its internal magnetizing current density is $\boldsymbol{J}_m=\nabla\times\boldsymbol{M}=0$, while the surface magnetizing currents density is [20]

$$\boldsymbol{K}_m=\boldsymbol{M}\times\hat{\boldsymbol{n}}, \quad (9)$$

where $\hat{\boldsymbol{n}}$ is surface normal unit vector.

By using the Biot-Savart law, the magnetic induction intensity $\boldsymbol{B}$ of an arbitrary point P in the space produced by a current can be calculated as

$$\boldsymbol{B}=\int_L\frac{\mu_0 I}{4\pi}\frac{d\boldsymbol{l}\times\boldsymbol{r}}{r^3}, \quad (10)$$

where the equivalent current $I=S\boldsymbol{K}_m$, S represents the area of the surface where the current exists, L is the path of integration, $d\boldsymbol{l}$ is the element of magnetizing current, $\boldsymbol{r}$ represents the vector pointing to P from the current element and μ_0 is the permeability of vacuum.

The system could be regarded as a model where one magnet A of the pair is placed in the external magnetic field produced by the other magnet B.

3.2.1. Cuboid magnets

For a cuboid magnet, we establish a Cartesian coordi-

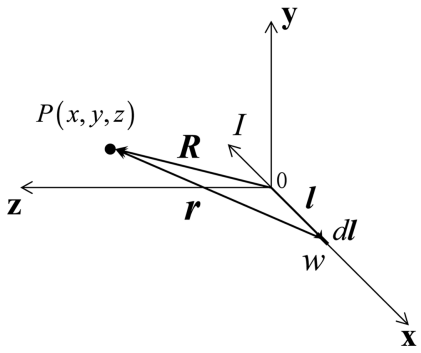

Fig. 8. Coordinate system of magnetic field produced by a current.

nate system as shown in Fig. 8. There is a current I along $\boldsymbol{x}$ axis pointing to the negative direction. $\boldsymbol{R}$ denotes a vector from the origin to the arbitrary point $P(x, y, z)$.

That is

$$\boldsymbol{R} = x\boldsymbol{i} + y\boldsymbol{j} + z\boldsymbol{k} \ , \tag{11}$$

$$\boldsymbol{L} = w\boldsymbol{i},\ d\boldsymbol{L} = -dw\boldsymbol{i}, \tag{12}$$

$$\boldsymbol{r} = \boldsymbol{R} - \boldsymbol{L} = (x-w)\boldsymbol{i} + y\boldsymbol{j} + z\boldsymbol{k} \ , \tag{13}$$

$$d\boldsymbol{L}\times\boldsymbol{r} = \begin{vmatrix} \boldsymbol{i} & \boldsymbol{j} & \boldsymbol{k} \\ -dw & 0 & 0 \\ x-w & y & z \end{vmatrix} = zdw\boldsymbol{j} - ydw\boldsymbol{k} \ , \tag{14}$$

$$r^3 = \left[(x-w)^2 + y^2 + z^2\right]^{\frac{3}{2}}. \tag{15}$$

For ease of magnetic induction intensity calculation, the coordinate system is established in which the magnet B is chosen to be the original point, as shown in Fig. 9. The direction of magnetization intensity $\mathbf{M}_B$ is along the axis $\boldsymbol{z}$.

The surface magnetizing current $I = l_B \int_L K_{mB} = l_B M_B$ is

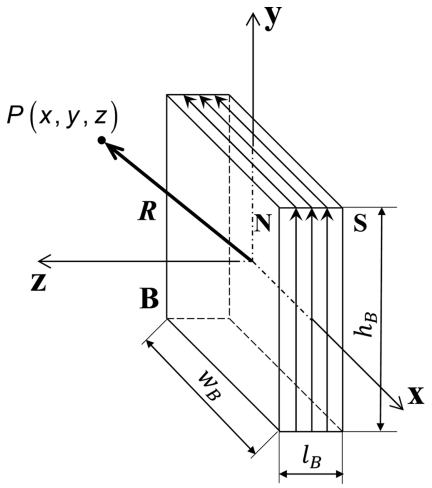

Fig. 9. Schematic diagram of magnet B's magnetizing currents

achieved from Eq. (9), where l_B, w_B and h_B shown in Fig. 9 have the same meaning as that in Fig. 4. Then, through transforming the coordinates and accumulating the magnetic field produced by the currents on the top, bottom, front and back surfaces, the magnetic induction intensities $\boldsymbol{B}$ of an arbitrary point P in x, y and z directions produced by magnet B are respectively achieved as

$$B_i(x,y,z) = \frac{\mu_0 M_B}{4\pi}\int_{-\frac{l_B}{2}}^{\frac{l_B}{2}} dz_0 \left\{ \int_{-\frac{w_B}{2}}^{\frac{w_B}{2}} \frac{(z-z_0)dv}{\left[\left(x-\frac{w_B}{2}\right)^2 + (y-v)^2 + (z-z_0)^2\right]^{\frac{3}{2}}} + \int_{-\frac{w_B}{2}}^{\frac{w_B}{2}} \frac{-(z-z_0)dv}{\left[\left(x+\frac{w_B}{2}\right)^2 + (y-v)^2 + (z-z_0)^2\right]^{\frac{3}{2}}} \right\}, \tag{16}$$

$$B_j(x,y,z) = \frac{\mu_0 M_B}{4\pi}\int_{-\frac{l_B}{2}}^{\frac{l_B}{2}} dz_0 \left\{ \int_{-\frac{h_B}{2}}^{\frac{h_B}{2}} \frac{(z-z_0)dw}{\left[(x-w)^2 + \left(y-\frac{h_B}{2}\right)^2 + (z-z_0)^2\right]^{\frac{3}{2}}} + \int_{-\frac{h_B}{2}}^{\frac{h_B}{2}} \frac{-(z-z_0)dw}{\left[(x-w)^2 + \left(y+\frac{h_B}{2}\right)^2 + (z-z_0)^2\right]^{\frac{3}{2}}} \right\}, \tag{17}$$

$$B_k(x,y,z) = \frac{\mu_0 M_B}{4\pi}\int_{-\frac{l_B}{2}}^{\frac{l_B}{2}} dz_0 \left\{ \int_{-\frac{h_B}{2}}^{\frac{h_B}{2}} \frac{-\left(x-\frac{w_B}{2}\right)dv}{\left[\left(x-\frac{w_B}{2}\right)^2 + (y-v)^2 + (z-z_0)^2\right]^{\frac{3}{2}}} + \int_{-\frac{h_B}{2}}^{\frac{h_B}{2}} \frac{\left(x+\frac{w_B}{2}\right)dv}{\left[\left(x+\frac{w_B}{2}\right)^2 + (y-v)^2 + (z-z_0)^2\right]^{\frac{3}{2}}} + \int_{-\frac{w_B}{2}}^{\frac{w_B}{2}} \frac{-\left(y-\frac{h_B}{2}\right)dw}{\left[(x-w)^2 + \left(y-\frac{h_B}{2}\right)^2 + (z-z_0)^2\right]^{\frac{3}{2}}} + \int_{-\frac{w_B}{2}}^{\frac{w_B}{2}} \frac{\left(y+\frac{h_B}{2}\right)dw}{\left[(x-w)^2 + \left(y+\frac{h_B}{2}\right)^2 + (z-z_0)^2\right]^{\frac{3}{2}}} \right\}, \tag{18}$$

The magnet A has the same size as magnet B, represented as l_A, w_A and h_A shown in Fig. 10. The magnetic

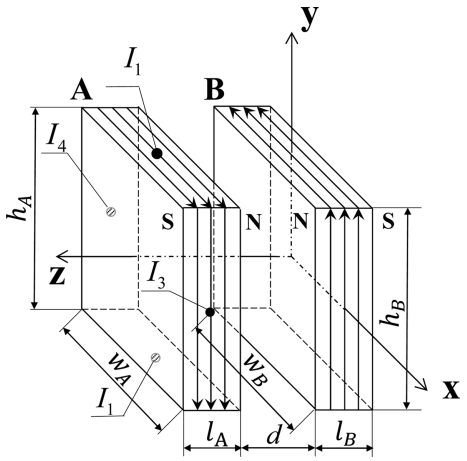

Fig. 10. The positions of magnetizing currents on the surfaces of magnet A in the coordinate system.

force can be equivalent to Ampere force of magnetizing currents on magnet A's surfaces [21].

$$\begin{aligned}\boldsymbol{F} &= -\iiint_V \boldsymbol{J}_{mA}\times\boldsymbol{B}dv - \iint_S \boldsymbol{K}_{mA}\times\boldsymbol{B}ds \\ &= -\iint_S \boldsymbol{K}_{mA}\times\boldsymbol{B}ds\end{aligned}. \tag{19}$$

Figure 10 shows the positions of magnetizing currents on the surfaces of magnet A in the coordination system. The coordinates on the centers of the top, bottom, front and back surfaces are respectively $I_1(x, y+\frac{h_A}{2}, z)$, $I_2(x, y-\frac{h_A}{2}, z)$, $I_3(x+\frac{w_A}{2}, y, z)$ and $I_4(x-\frac{w_A}{2}, y, z)$, where $z = d+\frac{l_B}{2}+\frac{l_A}{2}+z_1$ and d is the interval between two magnets.

Consequently, the interacting magnetic force between two cuboid magnets is

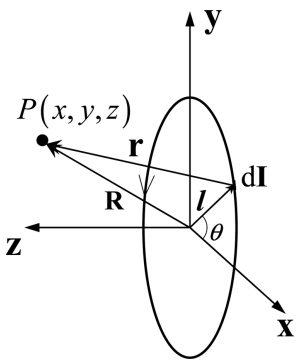

Fig. 11. Coordinate system of magnetic field produced by a circular current loop.

$$\begin{aligned}\boldsymbol{F}(x,y,z) = &\int_{-l_A/2}^{l_A/2}\left[\begin{aligned}&-\int_{-\frac{h_A}{2}}^{\frac{h_A}{2}} M_A B_k\left(x+\frac{w_A}{2}, y, z+z_1\right)dy \\ &+\int_{-\frac{h_A}{2}}^{\frac{h_A}{2}} M_A B_k\left(x-\frac{w_A}{2}, y, z+z_1\right)dy\end{aligned}\right]dz_1\boldsymbol{i} \\ &\int_{-l_A/2}^{l_A/2}\left[\begin{aligned}&-\int_{-\frac{w_A}{2}}^{\frac{w_A}{2}} M_A B_k\left(x, y+\frac{h_A}{2}, z+z_1\right)dx \\ &+\int_{-\frac{w_A}{2}}^{\frac{w_A}{2}} M_A B_k\left(x, y-\frac{h_A}{2}, z+z_1\right)dx\end{aligned}\right]dz_1\boldsymbol{j} \\ &\int_{-l_A/2}^{l_A/2}\left[\begin{aligned}&\int_{-\frac{w_A}{2}}^{\frac{w_A}{2}} M_A B_j\left(x, y+\frac{h_A}{2}, z+z_1\right)dx \\ &-\int_{-\frac{w_A}{2}}^{\frac{w_A}{2}} M_A B_j\left(x, y-\frac{h_A}{2}, z+z_1\right)dx \\ &+\int_{-\frac{h_A}{2}}^{\frac{h_A}{2}} M_A B_i\left(x+\frac{w_A}{2}, y, z+z_1\right)dy \\ &-\int_{-\frac{h_A}{2}}^{\frac{h_A}{2}} M_A B_i\left(x-\frac{w_A}{2}, y, z+z_1\right)dy\end{aligned}\right]dz_1\boldsymbol{k}\end{aligned}. \tag{20}$$

3.2.2. Cylindrical magnets

For a pair of cylindrical magnets, the basic theory of equivalent magnetizing current to calculate the interacting magnetic force is the same as cuboid magnets. There are circular current loops around the outermost cylindrical surface. Figure 11 shows the coordinate system in which the magnetic field is generated by a circular current loop.

According to Biot-Savart law, the magnetic induction intensity $\boldsymbol{B}$ from a circular current loop is calculated as follows:

$$\boldsymbol{B} = \int_L \frac{\mu_0 I}{4\pi}\frac{d\boldsymbol{l}\times\boldsymbol{r}}{r^3}, \tag{21}$$

$$\boldsymbol{R} = x\boldsymbol{i} + y\boldsymbol{j} + z\boldsymbol{k}, \tag{22}$$

$$\boldsymbol{l} = l\cos\theta\boldsymbol{i} + l\sin\theta\boldsymbol{j},\ d\boldsymbol{l} = -l\sin\theta d\theta\boldsymbol{i} + l\cos\theta d\theta\boldsymbol{j}, \tag{23}$$

$$\boldsymbol{r} = \boldsymbol{R} - \boldsymbol{l} = (x-w)\boldsymbol{i} + (y-v)\boldsymbol{j} + z\boldsymbol{k}, \tag{24}$$

$$\begin{aligned}d\boldsymbol{l}\times\boldsymbol{r} = &\, zl\cos\theta d\theta\boldsymbol{i} + zl\sin\theta\boldsymbol{j} \\ &-\left[l\sin\theta d\theta(y-l\sin\theta) + l\cos\theta d\theta(x-l\cos\theta)\right]\boldsymbol{k}\end{aligned}. \tag{25}$$

Therefore, the magnetic induction intensity of an arbitrary point $P(x, y, z)$ in space produced by cylindrical magnet B is derived by Eq. (21)-(25) and has the following form:

$$\begin{aligned}\boldsymbol{B} = \frac{\mu_0 M_B}{4\pi}\int_{-l_B/2}^{l_B/2} dz_0 \int_0^{2\pi}\Bigg(&\frac{(z-z_0)l\cos\theta}{r^3}d\theta\boldsymbol{i} + \frac{(z-z_0)l\sin\theta}{r^3}d\theta\boldsymbol{j} \\ &-\frac{(y-l\sin\theta)l\sin\theta + (x-l\cos\theta)l\cos\theta}{r^3}d\theta\boldsymbol{k}\Bigg)\end{aligned}, \tag{26}$$

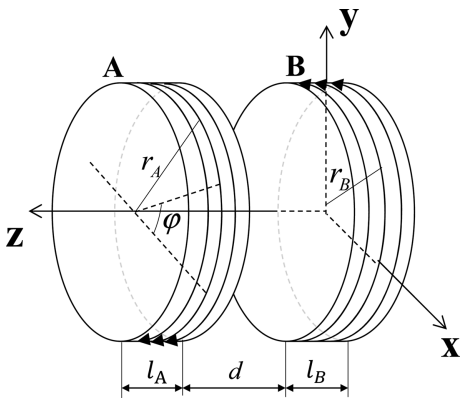

Fig. 12. The positions of magnetizing currents on the surface of magnet A in the coordinate system.

where $r^3=\left((x-l\cos\theta)^2+(y-l\sin\theta)^2+(z-z_0)^2\right)^{3/2}$, $l=r_B$ denotes the radius of magnet B, and l_B is the thickness of magnet B.

Consequently, the magnetic force between cylindrical permanent magnets can also be treated as the Ampere`s force. The coordinate system is shown in Fig.12 and the expressions of the force is achieved as:

$$\begin{aligned}\boldsymbol{F}=&\left[M_A r_A\int_{-l_A/2}^{l_A/2}dz_1\int_0^{2\pi}B_k\left(x+r_A\cos\varphi,y+r_A\sin\varphi,d+\frac{l_A}{2}+\frac{l_B}{2}+z_1\right)\cos\varphi d\varphi\right]\boldsymbol{i}\\&+\left[M_A r_A\int_{-l_A/2}^{l_A/2}dz_1\int_0^{2\pi}B_k\left(x+r_A\cos\varphi,y+r_A\sin\varphi,d+\frac{l_A}{2}+\frac{l_B}{2}+z_1\right)\sin\varphi d\varphi\right]\boldsymbol{j}\\&+\left[M_A r_A\int_{-l_A/2}^{l_A/2}dz_1\int_0^{2\pi}B_i\left(x+r_A\cos\varphi,y+r_A\sin\varphi,d+\frac{l_A}{2}+\frac{l_B}{2}+z_1\right)\cos\varphi d\varphi\right.\\&\left.+M_A r_A\int_{-l_A/2}^{l_A/2}dz_1\int_0^{2\pi}B_j\left(x+r_A\cos\varphi,y+r_A\sin\varphi,d+\frac{l_A}{2}+\frac{l_B}{2}+z_1\right)\sin\varphi d\varphi\right]\boldsymbol{k}\end{aligned},\tag{27}$$

where d still denotes the interval between permanent magnets.

4. Simulation and Comparison

In order to test and compare the magnetic force calculation accuracies of the two models, we simulate the interacting axial and lateral forces when one magnet is moving over another along the x-axis. The lateral force`s direction defined in this paper is the same as the moving direction. (In this paper, we only use symmetrical permanent magnets with square or circular pole face, so the directions of the movements and definition of the lateral force in y-axis will bring about the same result.) Besides, the displacement of the moving magnet is defined as zero when the projections of the pair of magnets coincide, as shown in Fig. 13, where magnet A is fixed and magnet B is movable. Next, we compare experimental measurements

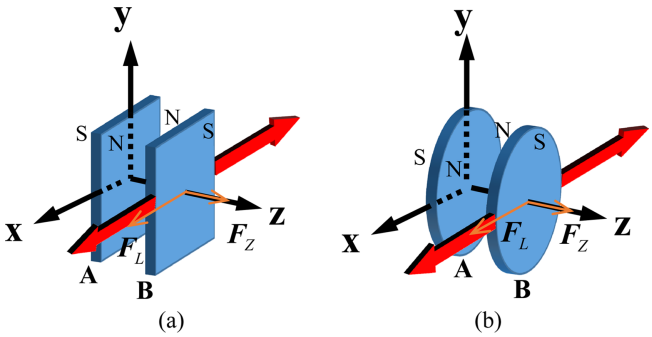

Fig. 13. (Color online) Schematic of the magnets moving state in the experiment and simulation. (a) cuboid magnets. (b) cylindrical magnets.

in Sec. II with the simulated axial and lateral magnetic forces as a function of the displacement x.

Table 1 shows the comparison between measured data in Sec. II and simulation results from two calculation models for magnets of two shapes in Sec. III. In the simulation, the sizes of magnets are referred to the real magnet's sizes in Sec. II, the interval d is set as 3 mm, the permeability of vacuum $\mu_0=4\pi\times10^{-7}$ H/m. The AF and LF in labels of figures are abbreviation for the axial magnetic force and lateral magnetic force.

It should be noted that the magnetizations intensities M are independent of integrals comparing different calculation expressions of magnetic force models, which means it could be put in the head or end of the formula as constants for uniformly magnetized permanent magnets. The value of magnetization intensity makes no difference in the general shape of simulation curve as a function of any abscissa parameter x or d because of the linear relationship between magnetization intensity and interacting magnetic force. It only influences the magnitude of magnetic forces.

Therefore, we assign the values of magnetization based on empirical criterions in the former researches and literatures to make the most of measured values consistent with the curves.

Concretely, we calculate the variances of absolute error between every simulated and measured value with different magnetization intensity. By comparing the variances:

$$Var=\frac{\sum_{i=1}^{N}(\Delta F_i)^2}{N},\tag{28}$$

we confirm the final magnetization intensity's value when the variance is minimum. The ΔF_i in the Eqn. (28) represents the absolute error of every force's value and is given by $\Delta F_i=F_{ei}-F_{si}(M)$, where F_{ei}, F_{si} and N represent the measured value, simulated value and the quantity of the

Table 1. Comparison of simulation results of two calculation models with the experiment data (displacements along x-axis change).

	Equivalent magnetic charge model	Equivalent magnetizing current model
Cuboid magnets	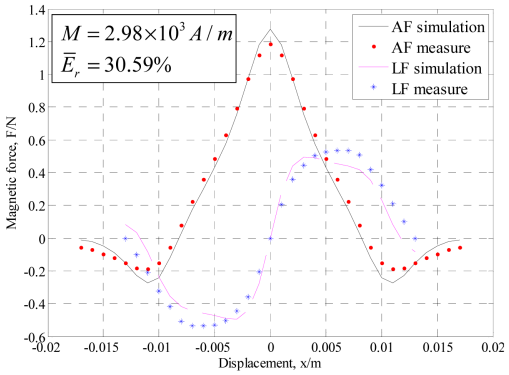	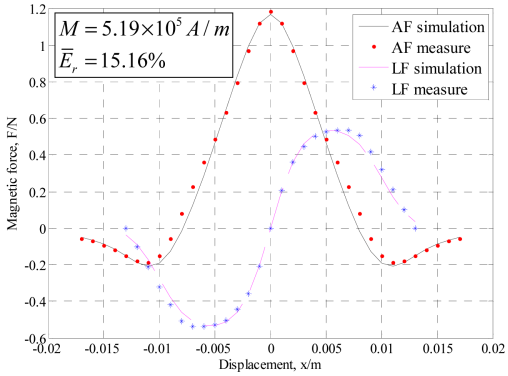
Cylindrical magnets	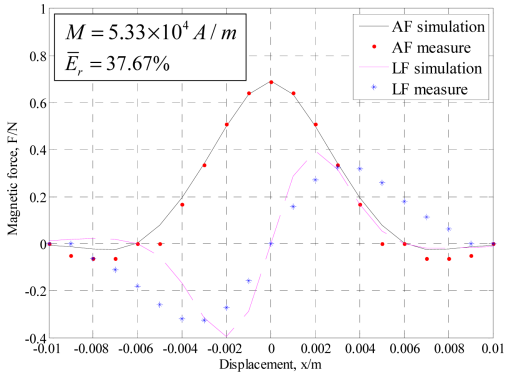	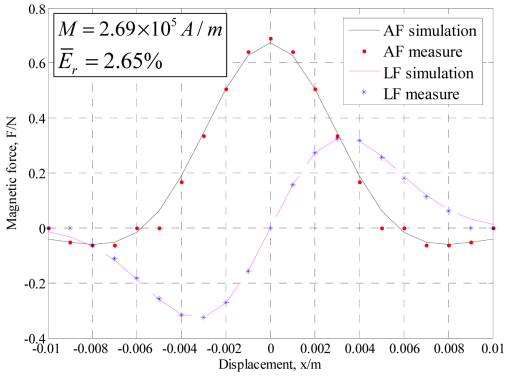

values which contains both axial and lateral forces. The minimum variance means the best agreement between experiment and simulation with the achieved magnetization intensity. The values of magnetization assigned in above several cases are different and marked in the figures of tables.

Then, we calculate the average relative errors:

$$\bar{E}_r = \frac{\sum_{i=1}^{N}\left|\frac{\Delta F_i}{F_{ei}}\right|}{N}, \tag{29}$$

excluding values of magnetic force smaller than 0.05N, which cannot be measured because of the zero-drift error of the dynamometer in the experiment. The results of each case are also marked in the figures. It can be proved that the accuracy of the equivalent magnetizing current model is higher than that of magnetic charge model with the average relative errors achieved.

In order to further verify the higher advantageous performance of the equivalent magnetizing current model, the interacting axial magnetic forces with several different intervals between magnets are simulated and measured when the projections of magnets coincide. The figures in Table 2 compare the experimental measurements with simulated axial magnetic forces as a function of the interval d. In a similar way, the average relative errors and magnetization intensities are also marked. The values of magnetization intensity are same as those of the cases in Table 1.

Here in Table 2, the calculation results of equivalent magnetizing current model also coincide well with that of experiment. No matter with visual judgement or comparison between average relative errors calculated and marked in the figures, the calculation accuracy of equivalent magnetizing current model is further proved to be much higher than that of equivalent magnetic charge model.

5. Analysis on the Equivalence between Two Models

Some researchers have mentioned the equivalence of the magnetic charge model and magnetizing current model and given their verification [17, 22]. But this equivalence is only studied at the micro scale. Considering the distribution of magnetic field produced by one magnetic dipole and a micro magnetizing loop current, or the acting force in the field, the expressions of the two models have the same form. We have calculated the magnetic field intensity produced by one magnetic charge as Eq. (2). The magnetic induction intensity produced by a micro

Table 2. Comparison of simulation results of two calculation models with the experiment data (intervals change).

	Equivalent magnetic charge model	Equivalent magnetizing current model
Cuboid magnets	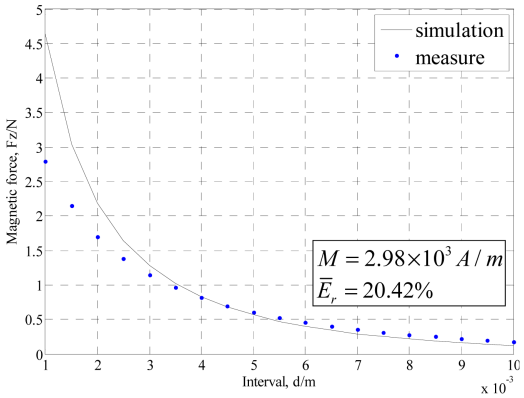	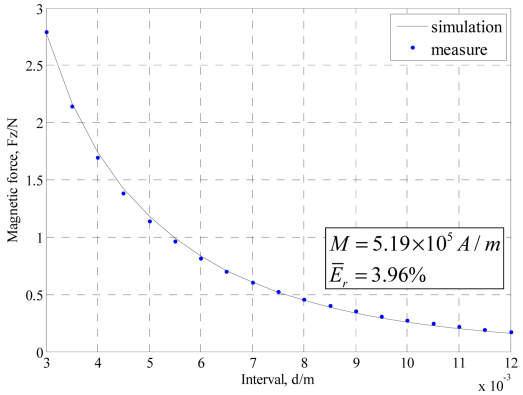
Cylindrical magnets	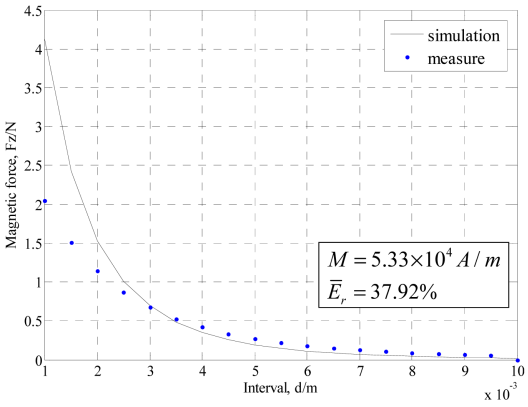	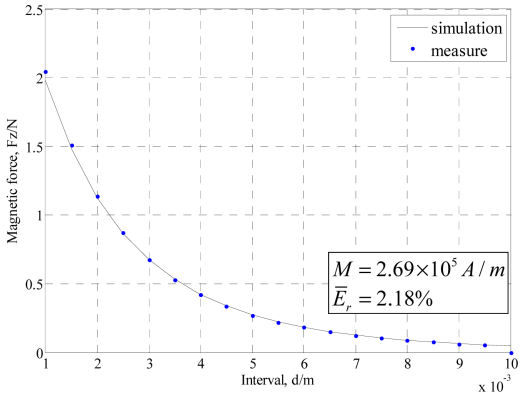

coil (magnetizing loop current) is $\boldsymbol{B} = \frac{\mu_0 I}{4\pi}\nabla\boldsymbol{\Omega}$, where Ω represents the solid angle subtended by the micro coil to a point $P(x, y, z)$ in the space, and $\Omega = \frac{Sz}{(x^2+y^2+z^2)^{3/2}}$ as shown in Fig. 14. Therefore, the magnetic induction intensities in three directions are achieved as following form:

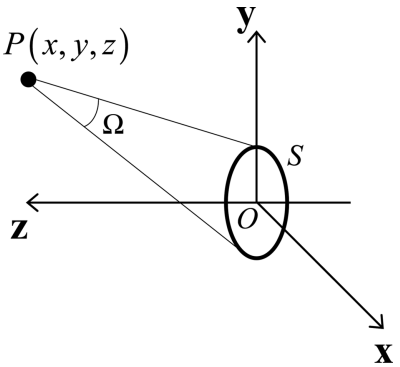

Fig. 14. The coordinate system of the field produced by a micro coil.

$$\begin{aligned} B_x &= -\frac{\mu_0 I}{4\pi}\frac{\partial\Omega}{\partial z} = -\frac{\mu_0 IS}{4\pi}\frac{3xz}{(x^2+y^2+z^2)^{5/2}} \\ B_y &= -\frac{\mu_0 I}{4\pi}\frac{\partial\Omega}{\partial z} = -\frac{\mu_0 IS}{4\pi}\frac{3yz}{(x^2+y^2+z^2)^{5/2}} \\ B_z &= -\frac{\mu_0 I}{4\pi}\frac{\partial\Omega}{\partial z} = -\frac{\mu_0 IS}{4\pi}\frac{2z^2-y^2-x^2}{(x^2+y^2+z^2)^{5/2}} \end{aligned} \quad (30)$$

Hereinbefore we have mentioned $p_m = \sigma_m S$, and $I = m/S$ in the Eq. (30) could be understood as the magnetic moment per unit area. The Eq. (2) and (30) are equal to each other while the relations are established like

$$\boldsymbol{B} = \mu_0 \boldsymbol{H}, \quad (31)$$

$$\boldsymbol{p}_m = \mu_0 \boldsymbol{m}. \quad (32)$$

Equivalent magnetizing current model states that magnetization intensity M is the average molecular magnetic moment of the unit volume $\boldsymbol{M} = \frac{\sum \boldsymbol{m}}{\Delta V}$ [23].

Similarly, the acting force of a micro coil is given by Ampere's force $\boldsymbol{F} = \boldsymbol{K} \times \boldsymbol{B}$ using the magnetizing current model, where $\boldsymbol{K} = \boldsymbol{m} \times \hat{\boldsymbol{n}}$ has been mentioned in Eq. (9). For the magnetic charge model, the acting force of a charge is $\boldsymbol{F} = p_m \boldsymbol{H}$, see Eq. (3). The equality of the acting

force expressions could also be derived as same as the field expression using the relations of Eq. (31) and (32) [14].

In most cases of the magnetic force calculation, the permanent magnets are, however, at the macro scale. As this paper shows, the theory of equivalent magnetizing current states that there are macro currents distributing only around the outermost loop, while the internal currents are offset by each other. Therefore, the calculation method is a kind of line integral of the current path if the thickness of the magnet is a constant. Whereas the theory of equivalent magnetic charge believes that the calculation method is a kind of surface integral of the magnetic pole faces, because the positive and negative magnetic charges distribute uniformly on the magnetic pole surface of permanent magnets. Hence, these two models by which the magnetic force between macro permanent magnets is calculated have no equivalence on account of different integral paths in the calculation as demonstrated in Sec. III. From micro to macro models, there exist different amplifications per radius or side length of magnets between cross section area (surface integral path) and perimeter (line integral path) of magnets. The cross-section area is a quadratic function of radius or side length, whereas perimeter is a linear function. That is the reason why the calculation results of two models are different at the macro scale.

6. Conclusion

Taking magnet pairs of two kinds of typical shapes for examples as calculation objects, this paper detailedly demonstrates the procedures of interacting magnetic force calculations between permanent magnets with two popular methods, magnetic charge model and magnetizing current model. It is affirmed that the equivalent magnetizing current model has higher accuracy. Moreover, we prove that there is no equivalence existing between magnetic charge model and magnetizing current model in the case of permanent magnets with macro volumes because of different integral paths, although equivalence exists between a single magnetic charge and a micro current loop for the calculation of magnetic field and force.

Furthermore, the method based on the equivalent magnetizing current theory can be used to calculate magnetic field and force of magnets with any shapes. The basic principle is uniform except for different integral paths. Hence, lots of applications could refer to our work to solve the problems on magnetic force calculation, such as magnets in bearings, motors and some sensors, which are suggested for the future research.

Acknowledgement

This work was financially supported by the National Natural Science Foundation of China (Grant No. 51675370) and the Tianjin Research Program of Application Foundation and Advanced Technology (Grant No. 15JCZDJC32200).

References

[1] C. W. Kim and J. Y. Choi, J. Magn. **21**, 110 (2016).
[2] Y. Leng, D. Tan, J. Liu, Y. Zhang, and S. Fan, J. Sound Vib. **406**, 146 (2017).
[3] W. Wang, J. Cao, N. Zhang, J. Lin, and W. Liao, Energy Convers. Manag. **132**, 189 (2017).
[4] Y. Zhang, Y. Leng, D. Tan, J. Liu, and S. Fan, Acta Phys. Sin. **66**, 220502 (2017).
[5] A. N. Vučković, S. S. Ilić, and S. R. Aleksić, Electromagnetics **32**, 117 (2012).
[6] R. Teyber, P. V. Trevizoli, T. V. Christiaanse, P. Govindappa, I. Niknia, and A. Rowe, J. Magn. Magn. Mater. **442**, 87 (2017).
[7] H. S. Choi, I. H. Park, and S. H. Lee, IEEE Trans. Magn. **42**, 663 (2006).
[8] B. L. J. Gysen, K. J. Meessen, J. J. H. Paulides, and E. A. Lomonova, IEEE Trans. Magn. **46**, 39 (2010).
[9] P. Liang, F. Chai, Y. Bi, Y. Pei, and S. Cheng, J. Magn. Magn. Mater. **417**, 389 (2016).
[10] J. Liang, J. Magn. **23**, 35 (2018).
[11] L. H. D. Medeiros, G. Reyne, and G. Meunier, IEEE Trans. Magn. **35**, 1215 (1999).
[12] V. Lemarquand and G. Lemarquand, Magnetic Bearings, Theory and Applications. InTech (2010) pp 85-115.
[13] R. Ravaud, G. Lemarquand, and V. Lemarquand, IEEE Trans. Magn. **45**, 2996 (2009).
[14] M. Greconici, Z. Cvetkovic, A. Mladenovic, S. Aleksic, and D. Vesa, IEEE OPTIM 12th International conference, Brasov (2010) pp 197-201.
[15] A. N. Vučković, S. S. Ilić, and S. R. Aleksić, Electromagnetics **33**, 421 (2013).
[16] R. Muscia, Electromagnetics **32**, 8 (2012).
[17] H. Zan and M. S. Thesis, Xi'an University of Architecture and Technology, Xi'an (2008).
[18] M. F. J. Kremers, D. T. E. H. V. Casteren, J. J. H. Paulides, and E. A. Lomonova, IEEE 10th International Conference on Ecological Vehicles and Renewable Energies (2015) pp 1-7.
[19] N. Sadowski, Y. Lefèvre, M. Lajoiemazenc, and J. P. A. Bastos, J. Phys. III **2**, 859 (1992).
[20] J. S. Agashe and D. P. Arnold, J. Phys. D Appl. Phys. **41**, 1586 (2008).
[21] S. Bobbio, F. Delfino, P. Girdinio, and P. Molfino, IEEE Trans. Magn. **36**, 663 (2000).
[22] T. Kovanen, T. Tarhasaari, and L. Kettunen, IEEE Trans. Magn. **48**, 13 (2012).
[23] K. Zhao and X. Chen, Electromagnetism, 3nd ed., Higher Education Press, Beijing (2011) pp 383-393.